Polymer Bulletin (2023) 80:8819–8844
https://doi.org/10.1007/s00289-022-04483-w

ORIGINAL PAPER

Assessing the potential of galactomannan isolated from six varieties of *Cyamopsis tetragonoloba* L. for hydrogel formation and controlled drug delivery

Sheena Jobin Alooparampil[1] · **Jigna G. Tank**[1]

Received: 28 July 2022 / Revised: 19 September 2022 / Accepted: 21 September 2022 /
Published online: 28 September 2022

Abstract

In the present studies, polysaccharide was extracted from 6 varieties of *Cyamopsis tetragonoloba* L. and its potential to form hydrogel was evaluated. The hydrogel formation was not observed in Desi and Neelam 51 variety but it formed particulate matter. Parasiya 954 and Maharani 92 formed intact, sticky, and watery gel whereas Swati and Nylon 55 formed intact, dense, and sticky gel with high water absorbing and swelling property. The rheological analysis of hydrogels (C, Pr2A, Mh2A, Sw2A, & Ny2A) suggested that they had a weak, flexible network structure and behaved as dilatant shear thickening fluid. The strength of Ny2A and Sw2A was high as compared to C, Pr2A, and Mh2A. The FESEM, FTIR, and XRD analysis of drug-loaded hydrogels confirmed the formation of polymerization in intact and sticky hydrogels, porous morphology, entrapment of insulin in hydrogels, the stable structure of insulin is retained and its amorphous dispersion in hydrogels, respectively. The in vitro controlled drug release was evaluated from each hydrogel by using insulin as a model drug using the Korsmeyer-Peppas model. The controlled drug (insulin) release was observed in formulations C, Pr2A, Mh2A, Sw2A, Ny2A, and Mh3A whereas controlled drug release was not observed in formulations Pr3A, Sw3A, Ny3A.

Keywords *Cyamopsis tetragonoloba* L. guar gum · Galactomannan · Hydrogel · FTIR · XRD · FESEM · Drug release · Insulin

✉ Jigna G. Tank
jignagtank@gmail.com

[1] Department of Biosciences, Saurashtra University, Rajkot, Gujarat 360005, India

Introduction

Guar Gum (galactomannan) is an endosperm polysaccharide commonly found mostly in leguminous seeds such as *Cyamopsis tetragonoloba* L., Trigonella foenum-graecum, Ceratonia siliqua, Caesalpinia pulcherrima, Cassia fistula, and many other seeds. The galactomannan shares a similar basic structure in different plants, but molecular weight variation appears different in different plants due to the variation in the ratio of mannose and galactose [1]. The variation in the mannose and galactose ratio affects the basic properties like water solubility, thermal stability, adhesive property, and rheological properties of the galactomannan [2]. The galactosyl side groups present in the galactomannan control the interchain association, its solubility, and crystallization in water depending on the temperature [3]. Galactomannan has practical applications as thickening, binding, emulsifiers, and stabilizing agents in the industrial fields for the production of valuable pharmaceutical, biomedical, cosmetics, and food products.

Thakura et al. [4] suggested the application of the guar gum in the development of hydrogels. Hydrogels are suggested to have widespread applications in drug delivery, tissue engineering, soil water retention, preparation of contact lenses, disposable diapers, and pet foods [5]. Elsaeed et al. [6] suggested that even though guar gum is salt and temperature sensitive, the physical and chemical properties of guar gum can be altered through the matrix by incorporation of cross-linking with various non-ionic and ionic monomers. He used acrylamide (non-ionic monomer) to improve salt tolerance and acrylamido-2-methylpropane sulfonic acid (hydrophilic monomer which contains non-ionic and anionic groups) to increase the swelling capacity of guar gum. The vital monomers used for the preparation of hydrogels are acryl amide, hydroxyethyl methacrylate, 2-hydroxypropyl methacrylate, and methoxyl poly (ethylene glycol). The incorporation of non-ionic matrices increases the salt tolerances and ionic matrices increase water solubility, thermal stability, and the possibility to form the hydrogel. It is observed that the cross-linked hydrogels have a three-dimensional structure for water retention and this property is helpful in the broad range of applications such as drug delivery systems, agriculture, pharmaceuticals, tissue engineering, and regenerative medicines [7–13].

Galactomannan's mucoadhesive properties, antioxidant nature, gelling properties, enzymatic degradation, and broad regulatory acceptance facilitated it as a suitable material for pharmaceutical applications and drug delivery carriers [14]. Sullad et al. [15] suggested that, polysaccharides are potential sources for controlled release (CR) systems. The control release kinetics of drug entrapped hydrogels can be regulated by the water uptake and cross-linkage of various agents like hydroxypropyl methylcellulose, Na-carboxymethylcellulose, poly (vinyl alcohol), and derivatives of cellulose. Soppimath et al. [16] also suggested that interpenetrating and semi-interpenetrating polymers can be developed for the external stimulus–response. This type of polysaccharide polymer can be loaded for bioactive agent delivery systems like nifedipine. Palem et al. [17] suggested that the modified biopolymer-based galactomannan hydrogels can be used as a

controlled drug release system. Verma and Sharma [14] suggested that polysaccharides like guar gum-based micro/nanoparticle encapsulated or entrapped with drugs can be an effective oral drug delivery for various gastrointestinal tract diseases due to their painless, cost-effective, non-invasion, safe, and ease of administration. Guar gum-based multi-model therapeutic oral nano-platform was suggested by Kumar et al. [18] for colorectal cancer treatment as a capping agent in the vicinity of the affected region.

Hence, it is necessary to compare the characteristics of guar gum (galactomannan) present in endosperm of different varieties of *Cyamopsis tetragonoloba* L. and evaluate its potential to form an excellent quality hydrogel and control drug release system. In the present study, galactomannan-based cross-linked hydrogels were prepared from six varieties of *Cyamopsis tetragonoloba* L. (Desi, Neelam 51, Parasiya 954, Maharani 92, Swati and Nylon 55) and its quality was determined. The controlled drug release from each prepared hydrogel was evaluated using insulin as a model drug. The characterization of hydrogels and insulin stability were determined through XRD, FTIR and FESEM analysis for its property, formation and utility. The controlled delivery of insulin was analyzed through in vitro drug release studies and validating it with different drug release kinetic models.

Materials and methods

Extraction of guar gum

The six varieties of *Cyamopsis tetragonoloba* L. seeds (Nylon 55, Swati, Parasiya 954, Neelam 51, Maharani-92, and Desi variety) (Table 1 Supplementary data) were purchased from the certified agriculture Seed store, Gita Enterprises, Amreli. Seeds (10 gm) of each variety were thoroughly washed and then soaked in distilled water for 72 h for the separation of the endosperm. The endosperm was separated from the seeds manually. The total endosperm obtained from 10 gm of seeds was weighed and then mixed with the distilled water to crush using a mechanical grinder to prepare viscous homogenate. Further, polysaccharide was precipitated from the homogenate by adding an equal volume of methanol to it. The precipitated polysaccharide was collected by filtration and then fresh weight and dry weight of polysaccharide were noted.

Fourier transform infrared (FTIR) analysis

Fourier transforms infrared (FTIR) spectra of each polysaccharide isolated from different *Cyamopsis tetragonoloba* L. varieties were recorded in Burker Vector 22 spectrophotometer. Each sample was scanned at the range of 4000–500 cm^{-1} wavelength at room temperature [19].

X-rays diffraction analysis

To determine changes in the properties of polysaccharides isolated from different varieties of *Cyamopsis tetragonoloba* L. X-rays diffraction analysis of polysaccharides was conducted. The XRD was performed at the angle between 0 and 80° with the scan rate at 1° min^{-1} at 2θ using an X-ray diffractometer (Jenis Panalytical Empyrean diffractometer) [20]. The percent crystalline index of galactomannan was determined by using following formula:

$$\%\text{Crystallinity} = \frac{I_c}{I_c + I_a} \times 100 \tag{1}$$

where I_a and I_c are the integrated intensities corresponding to the amorphous and crystalline phases, respectively [21]

Preparation of hydrogel

Hydrogel preparation was done by following the method described by Paixão and de Carvalho [22] with some modifications. Hydrogel preparation was done from galactomannan which was isolated from endosperm of different varieties of *Cyamopsis tetragonoloba* L. It was prepared by two ways either in the presence or absence of NaCl. The finely powdered guar gum (2 gm) was allowed to soak in 200 ml of distilled water overnight. To the soaked guar gum, 3gm of boric acid and 10 ml of 40% NaCl solution were added subsequently and homogenized thoroughly. Then, gradually 1 N sodium hydroxide (200 µl) was added to the homogenate until the hydrogel formation was observed. The pH of the solution was checked simultaneously with the addition of NaOH to determine the exact pH required for the formation of a hydrogel. The wet weight of hydrogel was noted and then it was immersed in methanol for overnight to dehydrate it to note the dry weight. The hydrogels prepared in presence of NaCl were given the following formulation codes: Desi (D3A), Neelam 51 (N 3A), Parasiya 954 (Pr 3A), Maharani 92 (Mh 3A), Swati (Sw 3A), Nylon 55 (Ny 3A). The hydrogels prepared in absence of NaCl (40% NaCl solution was not added to these gels) were given the following formulation codes: Desi (D 2A), Neelam 51 (N 2A), Parasiya 954 (Pr 2A), Maharani 92 (Mh 2A), Swati (Sw 2A), Nylon 55 (Ny 2A).

Swelling properties of hydrogel

Swelling properties of hydrogels were determined by following the method described by Shabir et al. [23] with some modifications. The powder of hydrogel (2 gm) was soaked in 100 ml of distilled water for 24 h at room temperature. Both swelling ratio (q) and percentage swelling (% ES) were measured using formulae described by Shabir et al. [23].

$$q = M_s/M_0 \tag{2}$$

where M_s is the mass of swollen hydrogel at time t and M_o is the mass of dry hydrogel

$$\% \text{ ES} = \frac{M_{eq} - M_0}{M_{eq}} \times 100 \tag{3}$$

where M_{eq} is swollen gel mass at time of equilibrium, M_o shows dried mass. Hence, % ES was calculated.

Determination of sol–gel fraction

The gel fraction of each hydrogel was measured as follows:

$$\text{Gel fraction (hydrogel\%)} = \left(\frac{W_d}{W_i}\right) \times 100 \tag{4}$$

$$\text{Sol fraction} = 100 - \text{Gel fraction} \tag{5}$$

where W_i is the initial weight of the dried sample and W_d is the weight of the dried insoluble part of the sample after extraction with water [24, 25].

Porosity measurement

The Solvent replacement method was used to determine the porosity of hydrogels as per Lin and Lu [26]. The porosity was calculated from the following equation

$$\text{Porosity} = \frac{(M_2 - M_1)}{\rho V} \times 100 \tag{6}$$

where M_1 and M_2 are the mass of hydrogel before and after immersion in ethanol, respectively, p is the density of absolute ethanol and V is the volume of the hydrogel [27].

Rheological evaluation of hydrogels

The hydrogels with formulation code C, Mh2A, Pr2A, Ny2A, & Sw2A (2% Concentration) were selected for rheological analysis as they formed intact gel with high water-holding capacity and swelling property. The viscosity of hydrogels was determined using a rheometer (Anton Paar MCR301) having application RHEOPLUS/32 V3.31 21003958-33056. Flow curves were obtained, using a steady-state flow ramp at 0.01–1000 s^{-1} shear rate. The power-law model was used to describe the experimental flow curves of hydrogels with the formula: $\tau = k\gamma n$, where τ is the apparent viscosity ($Pa{\cdot}s^n$), k is the consistency index, and n is the flow behavior index. The linear viscoelastic range was determined from the strain/amplitude sweep by varying shear stress at a constant frequency of 1 Hz. Further, frequency sweep was

determined at constant deformation ($\gamma = 0.1\%$) within the linear viscoelastic region and varying the frequency of oscillation from 100 to 0.01 Hz [28].

Drug loading

Drug loading onto hydrogel was performed by soaking the dry powder of polysaccharide (0.2 gm) in 20 mL of drug solution (insulin dry powder (from Sigma-Aldrich) was dissolved in 25 mM HEPES buffer of pH 8.0 with a concentration of 13.9 mg/ml) for a period of 8 h at 4 °C temperature. After that, 0.3 gm of boric acid, 0.4 gm of NaCl, and gradually 200 µl of 1 N NaOH were added until intact hydrogel formed. NaCl was not added to the hydrogels prepared in absence of NaCl. The formed hydrogels were allowed to gradually dry in methanol by incubating it overnight [29].

Drug loading determination

The weight of the loaded hydrogel was taken and the initial weight of the unloaded hydrogel was excluded from it to determine the loaded drug.

$$\text{Amount of drug} = \text{WD} - \text{Wd} \tag{7}$$

$$\text{Drug loading}(\%) = \left[\frac{\text{WD} - \text{Wd}}{\text{Wd}}\right] \times 100 \tag{8}$$

where Wd and WD are the weight of dried hydrogels before and after immersion in drug solution, respectively [23].

Scanning electron microscopy of drug-loaded hydrogel

The surface morphology of drug-loaded hydrogel was determined using a scanning electron microscope (ZEISS EVO 18, CARL ZEISS MICROSCOPY (PENTA FET X 3). After fixing samples on stub hydrogel were examined under an electron microscope [30].

Fourier transform infrared (FTIR) analysis of drug-loaded hydrogels

Fourier transforms infrared (FTIR) spectra of insulin solution and drug-loaded hydrogels were recorded in Burker Vector 22 spectrophotometer. Each sample was scanned at the range of 4000–500 cm^{-1} wavelength at room temperature [19].

In vitro drug release

Each gel disk was placed in Tris–HCl buffer (pH-7.4) for 24 h, then the same disk was shifted in fresh Tris–HCl buffer (pH-7.4) after every 24 h, and release was observed for total of 120 h. Each sample was mixed with the Bradford reagent and

then optical density was measured at 595 nm [31]. To determine drug release, the following formula was used:

$$\%\text{Drug release} = \frac{\text{Ft}}{\text{Fload}} \times 100 \tag{9}$$

where Ft shows the quantity of Insulin released at any time t and Fload represents the quantity of insulin that was loaded in the hydrogel matrix. The drug release kinetics was evaluated by data modeling using DD solver software for data analysis [30].

Statistical analysis

All the measured quantitative and qualitative parameters (yield of hydrogel, water-holding capacity, swelling property, sol–gel fraction, porosity, and drug loading capacity) of all 12 hydrogels were subjected to Multivariate cluster analysis to construct a dendrogram based on the similarity matrix data using the paired group (UPGMA) method with arithmetic averages and the Bray–Curtis similarity index. Non-metric multidimensional scaling was done to group all the six hydrogels on the basis of similarity in quantitative and qualitative parameters. These analyses were performed using PAST: Palaeontological Statistics software package version 4.05 [32].

Results and discussion

Yield of polysaccharide

In the present studies, polysaccharides were isolated from six varieties of *Cyamopsis tetragonoloba* L. The yield of polysaccharides obtained from the Desi variety was 80.08%, Neelam 51 variety was 62.29%, Parasiya 954 variety was 48.54%, and Maharani 92 variety was 94.82%, Swati variety was 26.28%, and Nylon 55 variety was 51.90%. Among all the six varieties, the highest yield of polysaccharides was obtained from Maharani 92 variety and the lowest yield of polysaccharides was obtained from the Swati variety (Fig. 1 Supplementary data).

FTIR analysis of polysaccharide

The FTIR spectra and peaks of galactomannan (isolated from different varieties of *Cyamopsis tetragonoloba* L.) were compared with the FTIR data of galactomannan given by Mudgil et al. [33] it was observed that there was a remarkable change in the bond pattern of galactomannan isolated from each variety. Galactomannan isolated from the Nylon 55 variety had OH stretching vibration which was not observed in galactomannan isolated from other varieties. The galactomannan isolated from the Swati variety had N–H stretching vibration (free), C H stretching vibrations, and CC stretching vibration which was not observed in galactomannan isolated from

other varieties. The galactomannan isolated from Parasiya 954, Maharani 92, Swati, and Nylon 55 had C H stretching of CH_2 group which was not observed in galactomannan isolated from Desi and Neelam 51 variety. The galactomannan isolated from Desi and Neelam 51 variety had αβ unsaturated, C–H out-of-plane deformation vibration which was not observed in other varieties. The galactomannan isolated from Swati and Nylon 55 variety had CH_2 twisting vibration which was not observed in other varieties. The Ring stretching of Galactose & mannose and Symmetrical deformations of CH_2 group was observed in galactomannan isolated from all the varieties. The C=O stretching vibration was observed in galactomannan isolated from Desi, Neelam 51 and Maharani 92 variety which was not observed in Parasiya 954, Swati, and Nylon 55 variety. The FTIR spectra of galactomannan isolated from Desi and Neelam 51 variety were similar to each other. The FTIR spectra of galactomannan isolated from Parasiya 954 and Maharani 92 variety were similar to each other. The FTIR spectra of galactomannan isolated from Swati and Nylon 55 variety were similar to each other (Fig. 2, Table 2 Supplementary data).

In present studies, there was a remarkable difference in the chemical characteristics of galactomannan which influenced hydrogel formation from different varieties of Cyamopsis tetragonoloba L. The hydrogel formation was not observed from Desi and Neelam51 varieties whereas the hydrogel formation were observed from Parasiya 954, Maharani 92, Swati, and Nylon 55. This was due to the change in the bond pattern of all the polysaccharides. The characteristic O–H stretching, C H stretching of CH2 group, CH2 twisting vibration in the galactomannan of Parasiya 954, Maharani 92, Nylon 55, and Swati variety is due to the presence of acidic fraction [34] which allows the formation of an intact and sticky gel. However, the absence of these groups in the Desi and Neelam 51 variety results in the formation of a particulate matter. In previous studies, it is being suggested that the peaks in the FTIR spectra between 800 and 1200 cm^{-1} represent the stretching of C–C–O, C–OH, and C–O–C polymer backbone [35]. The peak around 1400 cm^{-1} is due to the Symmetrical deformations of CH2 group [36]. The peak around 1650 cm^{-1} is due to the ring stretching [33]. The peak in the FTIR spectra around 2885 and 2943 cm^{-1} is due to C–H stretching vibrations of CH2 group of galactomannan [33, 37]. The peak in the FTIR spectra around 3151–3587 cm^{-1} is due to O–H stretching vibrations of hydrogen bond formed between polymer and water [33, 37, 38].

X-ray diffraction of polysaccharide

The X-ray diffraction pattern of galactomannans isolated from different *Cyamopsis tetragonoloba* L. varieties revealed that all the isolated galactomannans presented an amorphous structure. The X-ray diffraction pattern of galactomannan isolated from Desi and Neelam 51 variety was similar to each other. The crystalline region of galactomannan isolated from Desi and Neelam 51 variety was seen at the angle (2θ) 22.21 and 22.53, respectively. The crystallinity index calculated from galactomannan of Desi and Neelam 51 variety was 2.69 and 2.01%, respectively. The X-ray diffraction pattern of galactomannan isolated from Parasiya 954 and Maharani 92 variety was similar to each other. The crystalline region

of galactomannan isolated from Parasiya 954 and Maharani 92 variety was seen at the angle (2θ) 22.97 and 23.08, respectively. The crystallinity index calculated from galactomannan of Parasiya 954 and Maharani 92 variety was 3.44 and 3.84%, respectively. The X-ray diffraction pattern of galactomannan isolated from the Swati and Nylon 55 variety was similar to each other. The crystalline region of galactomannan isolated from the Swati and Nylon 55 variety was seen at the angle (2θ) 27.03 and 28.32, respectively (Fig. 1). The crystallinity index calculated from galactomannan of Swati and Nylon 55 variety was 4.18 and 3.70%, respectively. The X-ray diffraction pattern of food-grade galactomannan taken as reference was similar to the XRD pattern of Nylon 55 variety with crystalline region seen at the angle (2θ) 27.37. The crystallinity index of food-grade galactomannan was 3.87% which was almost nearer to the galactomannan of Parasiya 954, Maharani 92, Nylon 55, and Swati varieties.

In present studies, X-ray diffraction analysis of galactomannans isolated from different varieties of *Cyamopsis tetragonoloba* L. revealed that it has an amorphous structure. Similar results are also observed in previous studies carried out by Mudgil et al., Liyanage et al. [1, 39] after XRD analysis of native guar gum, guar galactomannan, and food-grade guar gum. As per the previous studies the crystalline region of galactomannan is usually seen approximately at the 2θ of 20.2. Similarly, in present studies, the crystalline region of galactomannan isolated from Desi (22.21°), Neelam 51 (22.53°), Parasiya 954 (22.97°), Maharani 92 (23.08) varieties of *Cyamopsis tetragonoloba* L. was nearer to the 2θ of 20.2°. However, the crystalline region of galactomannan isolated from Swati (27.03°) and Nylon 55 (28.32°) was higher than 20.2°. The Percent crystallinity index determines the alignment of molecules in particle structure. In present studies, the crystallinity index of galactomannan isolated from Parasiya 954 (3.44%), Maharani 92 (3.84%), Swati (4.18%), and Nylon 55 (3.70%) varieties were similar to the crystallinity index of food-grade galactomannan (3.87%) purchased from the market as well as crystallinity index of native guar gum (3.86%) determined by Mudgil et al. [39].

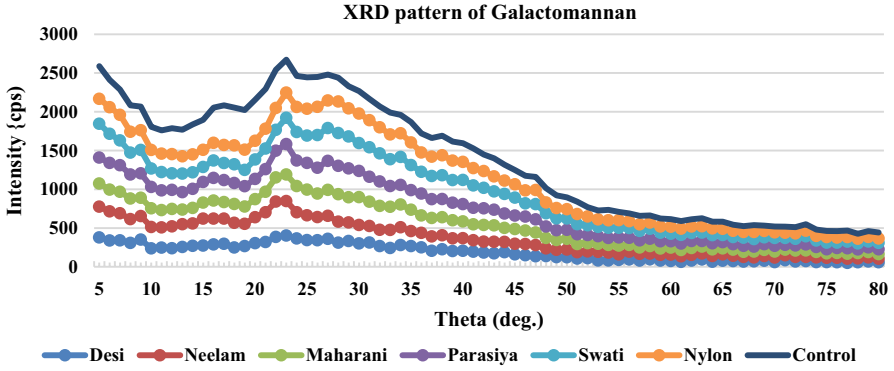

Fig. 1 XRD pattern of polysaccharide isolated from different *Cyamopsis tetragonoloba* L. varieties

Yield of hydrogel and its physiological changes due to pH

In present studies, the hydrogel was prepared from all the six varieties of *Cyamopsis tetragonoloba* L. by two ways: (1) Hydrogel preparation in presence of NaCl (by using boric acid, sodium chloride and sodium hydroxide) and (2) Hydrogel preparation in absence of NaCl (by using boric acid and sodium hydroxide). The yield of hydrogel obtained from Parasiya 954 and Maharani 92 variety in presence of NaCl was 96.75 and 96.77%, respectively. The yield of hydrogel obtained from Parasiya 954 and Maharani 92 variety in absence of NaCl was 98.94 and 96.10%, respectively. The yield of hydrogel obtained from Swati and Nylon 55 variety in presence of NaCl was 97.84 and 96.86%, respectively. The yield of hydrogel obtained from Swati and Nylon 55 variety in absence of NaCl was 99.08 and 99.16%, respectively. However, hydrogel formation was not observed from galactomannan of Desi and Neelam 51 variety whether prepared in the presence or absence of NaCl. It remained particulate matter with no water-holding and swelling properties.

Among the two ways used for the preparation of hydrogels from galactomannan, it was observed that the physiological properties of hydrogel can be altered in absence of NaCl. The hydrogels prepared in presence of NaCl directly form a thick, dense and intact gel when the pH of the solution reaches 7.5, the quantity of hydrogel is less and it has less water-holding capacity. However, hydrogel prepared in absence of NaCl can form different physiological forms such as watery hydrogel, thick watery hydrogel, and intact sticky hydrogel by altering the volume of NaOH which changes the pH from 6.5, 7, 7.5, 8, and 8.5, respectively (Table 3 Supplementary data). The quantity of this hydrogel is more and has a high water-holding capacity.

In previous studies, it is already observed that in presence of borate ions galactomannan forms gel at neutral or alkaline pH [40, 41]. Borate ions have hydroxyl groups which form several cross-links with polymers to impart gelling properties [40, 42]. The physiological forms of the hydrogel can be altered to watery hydrogel, thick watery hydrogel, or intact sticky hydrogel due to the gradual conversion of boric acid into borate anions with a change in pH from 6.5 up to 8.5 [43, 44]. The interaction between the hydroxyl group of borate ions and the cis-hydroxyl group of guar gum at pH 6.5–7.5 forms a 1:1 complex when the concentration of borate ions is low. However, at pH 8–11 it forms a 2:1 complex when the concentration of borate ions is high. The formation of the 2:1 complex has higher viscosity as compared to the 1:1 complex which results in a change in the physiological form of a hydrogel [44, 45].

Swelling property of hydrogels

From the swelling studies, it was observed that the swelling property of hydrogels D3A, D2A, N3A, and N2A was 0%. The swelling property of hydrogels Pr3A was 95% and Pr2A was 90.67%, respectively. The swelling property of hydrogels Mh3A was 94.3% and Mh2A was 55.22%, respectively. The swelling property of hydrogels

Sw3A was 92.93% and Sw2A was 87%, respectively. The swelling property of hydrogels Ny3A was 92.99% and Ny2A was 87.2%, respectively (Figs. 3 and 4 Supplementary data).

The water-holding property of hydrogels varied from each other due to the change in the characteristics of polysaccharides, the concentration of cross-linkers, and the pH of the formulation. The hydrogel prepared in absence of NaCl had high water-holding property due to the presence of boric acid that contains hydroxyl group which gets ionized with the increase in the pH of the formulation toward the basic environment due to the addition of NaOH. This results in ionization of hydroxyl group, an increase in osmotic pressure and electrostatic repulsion within the hydrogel causing the network to expand [30]. As the pH of the solution moves toward the basic condition the electrostatic repulsive force between the hydroxyl group of boric acid increases which in turn increases the water-holding capacity of the hydrogel and swells it [46–49].

Determination of sol–gel fractions in the hydrogels

The hydrogels which showed intactness, water-holding capacity, and swelling properties were further considered for the determination of sol–gel fractions. There was a remarkable influence of NaCl in gel and sol fraction of hydrogels prepared from Parasiya 954, Maharani 92. Swati and Nylon 55 varieties. The hydrogel Pr3A had 95% gel fraction and 5% sol fraction whereas hydrogel Pr2A had 90.67% gel fraction and 9.32% sol fraction. The hydrogel Mh3A had 94.31% gel fraction and 5.68% sol fraction whereas hydrogel Mh2A had 55.22% gel fraction and 44.77% sol fraction. The hydrogel Sw3A had 92.93% gel fraction and 7.06% sol fraction whereas hydrogel Sw2A had 87.54% gel fraction and 12.45% sol fraction. The hydrogel Ny3A had 92.99% gel fraction and 7.00% sol fraction whereas hydrogel Ny2A had 87% gel fraction and 13% sol fraction (Figs. 5 and 6 Supplementary data).

In all the hydrogel formulations (Pr2A, Pr3A, Mh2A, Mh3A, Sw2A, Sw3A, Ny2A, & Ny3A) the gel fraction was higher than the sol fraction whether it is prepared in the presence or absence of NaCl. The gel fraction was high because, with an increase in monomer and cross-linker concentration, there is an increase in cross-linking which in turn increases the strength of gel and its function [27]. It was observed that the physical properties of hydrogels prepared in presence of NaCl cannot be changed and it forms a direct intact sticky gel at pH 7.5–8. However, the physical properties of hydrogels prepared in absence of NaCl can be changed to watery hydrogel, thick watery hydrogel, or intact sticky hydrogel by adjusting the pH of formulation from pH 6–8.5. Even the porosity of hydrogels prepared in presence of NaCl was less as compared to the porosity of hydrogels prepared in absence of NaCl. This was due to the increase in molecular entanglement between polymer and monomer which increases cross-linking density, decreases pore formation and decreases the mesh size of hydrogen [27, 50]. As the concentration of cross-linker increases, cross-link points also increase which results in high cross-link density [51–53].

The porosity of the hydrogels

In hydrogel, Pr3A porosity was 70.97% whereas, in hydrogel Pr2A slight increase in porosity (76.04%) was observed. In hydrogel Mh3A porosity was 65.90% whereas in hydrogel Mh2A decrease in porosity (40.55%) was observed. In hydrogel, Sw3A porosity was 50.69% whereas a slight increase in porosity (53.23%) was observed in hydrogel Sw2A. In hydrogel, Ny3A porosity was 63.37% whereas a slight increase in porosity (70.97%) was observed in hydrogel Ny2A (Fig. 7 Supplementary data).

Rheological properties of hydrogel

The intact hydrogels (C, Pr2A, Mh2A, Sw2A, & Ny2A) of 2% concentration and pH 8.0 were used to develop steady shear flow curves. The high viscosities of all the hydrogels gradually decreased significantly with the varying shear rate from 0.01 to 1000 s^{-1}. This indicates the shear-thinning behavior of all the hydrogels (Fig. 2). The coefficients of determination (R^2) were higher than 0.91 for all tested samples which indicate the appropriateness of the power low model used to describe the flow properties of the hydrogels. The viscosity of all hydrogels was determined through shear stress versus shear rate ratio (Fig. 3) which revealed that all the hydrogels had constant viscosity at the low shear rate (Newtonian behavior), indicating the weak and flexible structure of all hydrogels.

From rheological analysis of hydrogels, it was observed that the high viscosity of all the hydrogels decreased gradually with an increase in the shear rate from 0.01 to 1000 S^{-1}. This was due to the breakdown of the network structure due to shear stress and the solution began to flow down showing the shear-thinning behavior. The viscosity of all hydrogel had Newtonian behavior which indicates weak and

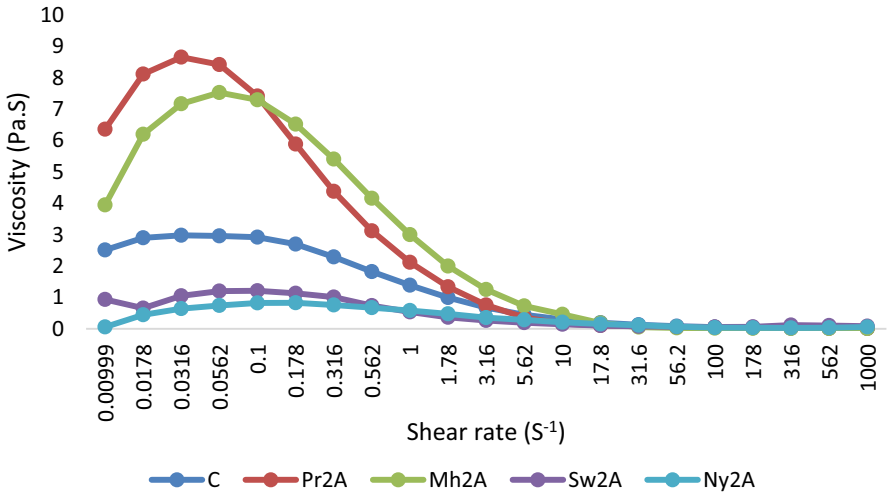

Fig. 2 Stear dependent viscosity measurements in hydrogels (C, Pr2A, Mh2A, Sw2A, Ny2A) at 25 °C

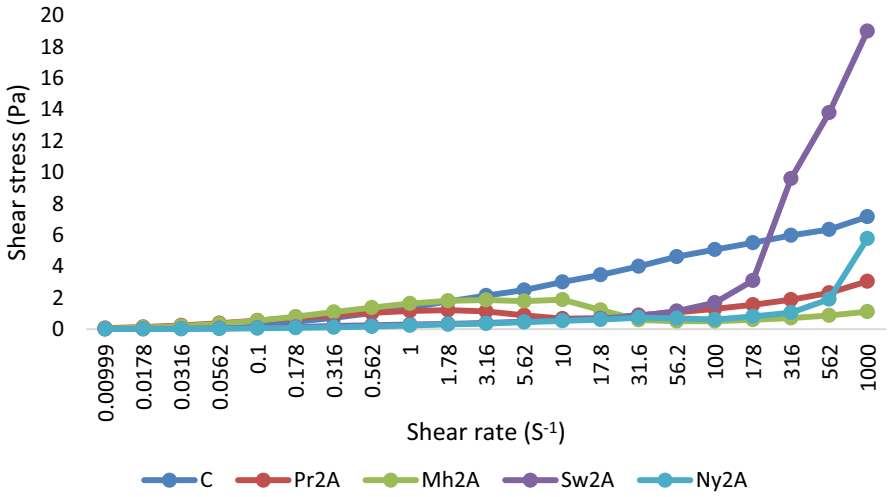

Fig. 3 Shear stress vs Shear rate measurements for hydrogels (C, Pr2A, Mh2A, Sw2A, Ny2A) at 25 °C

flexible structure of hydrogels which promotes entanglement of polymer chains. Similar shear-thinning behavior in hydrogels was also observed in previous studies on hydroxypropyl guar gum hydrogel [44], gelatin hydrogels [28], and Alginate based hydrogels [54]. In the present studies, all hydrogels were subjected to strain/amplitude sweep at a constant frequency to determine viscoelastic behavior and sol–gel transition of the hydrogel. The storage modulus indicates solid or elastic characteristic of the hydrogel and the loss modulus indicates the liquid-like or viscous behavior of the hydrogel. The combination of storage and loss modulus indicates viscoelasticity behavior as well as the sol–gel transition of the hydrogel [28]. In present studies, all the hydrogels had G' value higher than G" values that indicate high elasticity in borate cross-linked hydrogels. Similar results were also observed by Wang et al. [44] in hydroxypropyl guar gum hydrogel. The strength of the galactomannan network was determined through frequency sweep. In present studies, all hydrogels depicted loss modulus G' values higher than storage modulus G" values for the range of frequencies studied which depicts appearances of network structure [44]. The tan δ values determine the rigidity of the hydrogels, the higher tan δ value indicates more flexibility in hydrogel structure and low tan δ value indicates rigidity in hydrogel structure [55]. In present studies, tan δ values of Sw2A and Ny2A were slightly higher than the tan δ values observed in C, Pr2A, and Mh2A which indicates the strength of Ny2A and Sw2A varieties is higher as compared to C, Pr2A, and Mh2A.

The linear viscoelastic properties of all the hydrogels (C, Pr2A, Mh2A, Sw2A, & Ny2A) were studied by using the strain/ amplitude sweep. In the present studies, the flow point at which storage (G') and loss (G") modulus crossed in the control sample was $\gamma = 75.3\%$ strain. In Ny2A, the flow point at which storage (G') and loss (G") modulus crossed is 75.9% strain. In Sw2A, the flow point at which storage (G') and loss (G") modulus crossed is 19.1% strain. In Mh2A, the

flow point at which storage (G') and loss (G") modulus crossed is 77% strain. In Pr2A, the flow point at which storage (G') and loss (G") modulus crossed is 199% strain. In all the hydrogels, the viscous modulus (G″) prevailed over the elastic modulus (G′). There was a remarkable decrease in the G' and G" values in all the hydrogels with the increase in the amplitude from 0.1 to 1000%. This suggests that the hydrogel Sw2A remains in the linear viscoelastic domain for very short time with an increase in the amplitude (G' = G") around $\gamma = 19.1\%$. The hydrogels C, Ny2A, and Mh2A remain in the linear viscoelastic domain for short time with an increase in the amplitude (G' = G") around $\gamma = 75$–77%. However, the hydrogel Pr2A remains in the linear viscoelastic domain for longer with the increase in the amplitude (G' = G") around $\gamma = 199\%$ (Fig. 4). After that the elastic regime became dominant (G' > G") and the solution began to flow due to the breakdown

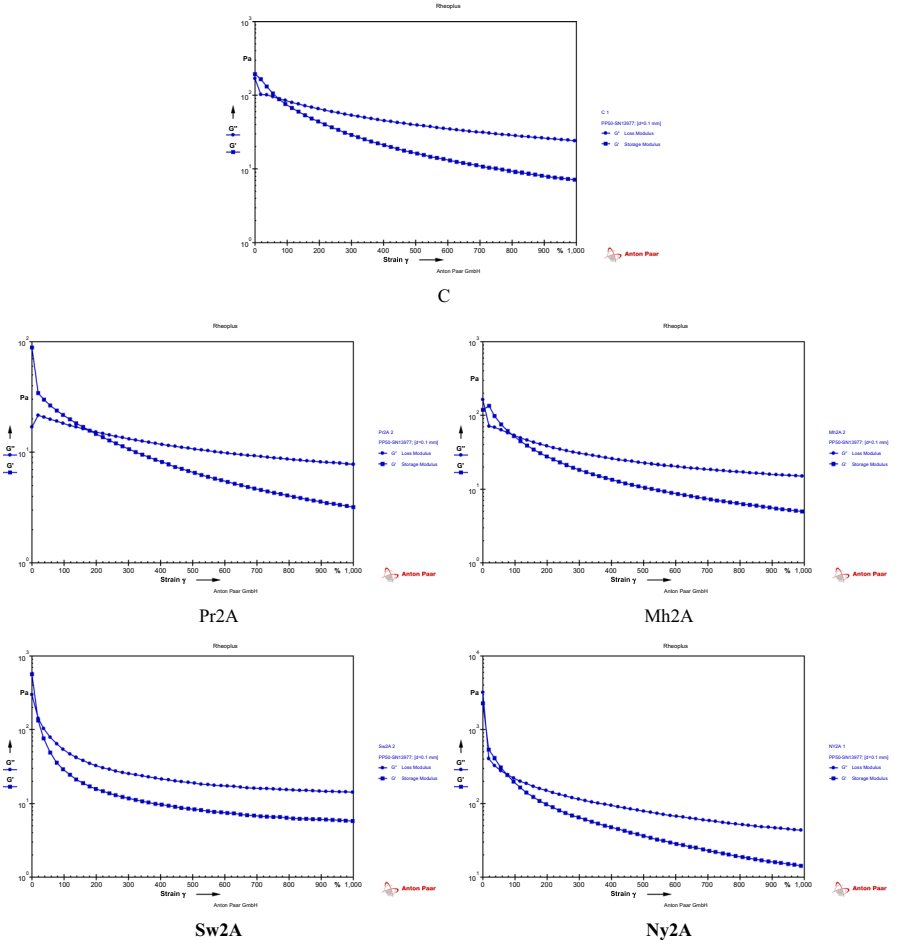

Fig. 4 Oscillatory amplitude sweeps at a constant frequency of oscillation of 1 Hz measurements for hydrogels (C, Pr2A, Mh2A, Sw2A, Ny2A) at 25 °C

of the network structure. This indicates network structure was generated and it began to behave as dilatant shear thickening fluid.

To study the strength of the hydrogel network, frequency sweep studies were performed in the range of 0.01–100 Hz. In control, the loss modulus G' values were higher than the storage modulus G" values for all frequencies which result in a relative increase in values of tan δ. Even there was increase in complex viscosity with an increase in the oscillation of frequency that confirms the increase in hydrogen bonds formation between the polymer, cross-linkers and the water molecules. Similar results were obtained in hydrogels Pr2A and Mh2A. However, in Ny2A and Sw2A hydrogels, the loss modulus G' values were slight higher than the storage modulus G" values for all frequencies which results in relative decrease in the values of tan δ. Here, there was decrease in complex viscosity with increase in oscillations of frequency that confirms the decrease in hydrogen bonds formation and stabilizes the structure of galactomannan macromolecules (Fig. 5). This indicates that the strength of Ny2A and Sw2A hydrogels is high as compared to the C, Pr2A, and Mh2A.

Drug loading studies

The amount of drug-loaded in the hydrogel Pr3A was 74.02% and Pr2A was 67.21%. The amount of drug-loaded in the hydrogel Mh3A was 78.02% and Mh2A was 83.60%. The amount of drug-loaded in the hydrogel Sw3A was 76.47% and Sw2A was 83.60%. The amount of drug-loaded in the hydrogel Ny3A was 84% and Ny2A was 82.14%. It was observed that the presence of NaCl is not affecting much the drug loading capacity of hydrogels (Fig. 8 Supplementary data).

FTIR analysis of drug-loaded hydrogels

To confirm the stability of the insulin within the hydrogel FTIR analysis of drug-loaded gel was carried out. The comparative analysis of FTIR spectra of insulin solution with the FTIR spectra of drug-loaded hydrogels confirmed that the entrapment of insulin solution in hydrogels with stable structure of insulin retained in it (Fig. 6, Table 4 Supplementary data).

Scanning electron microscopy of drug-loaded hydrogels

From FESEM analysis of drug-loaded hydrogels, it was observed that the insulin solution was trapped in the porous spaces of the hydrogel. Figure 7 depicts the porous spaces of hydrogels appeared open due to the trapping of insulin solution within them. All the prepared hydrogels showed the same characteristics.

X-ray diffraction of drug-loaded hydrogel

The X-ray diffraction pattern of hydrogels loaded with insulin supported the above FESEM results and revealed that the characteristic peaks of insulin were in galactomannan spectra of hydrogel with no change in diffraction pattern between

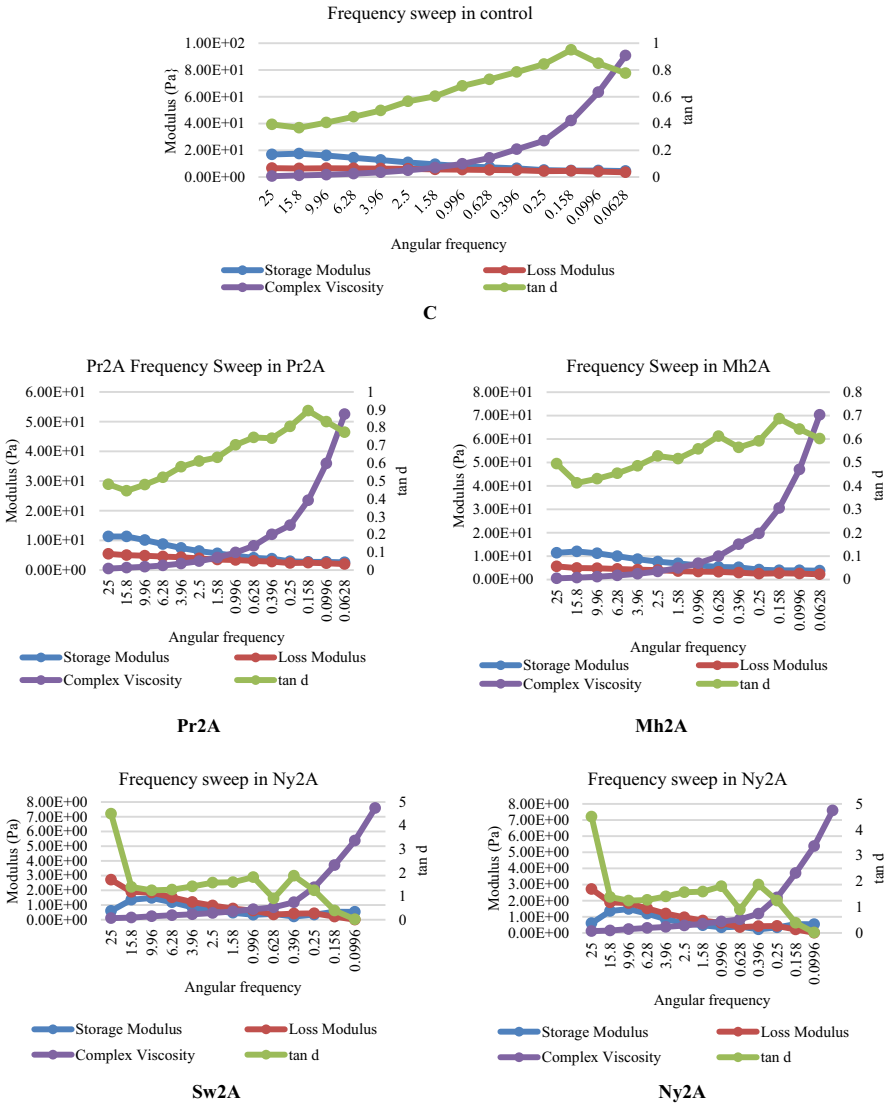

Fig. 5 Frequency sweep measurements in a linear viscoelastic range at the deformation of 0.25% for hydrogels (C, Pr2A, Mh2A, Sw2A, Ny2A) at 25 °C

two molecules. The crystalline region of insulin loaded control hydrogel (C) was seen at the angle (2θ) 20.18 and its crystallinity index was 3.69%. The crystalline region of insulin loaded Pr2A hydrogel was seen at the angle (2θ) 22.71 and its crystallinity index was 3.92%. The crystalline region of insulin loaded Pr3A hydrogel was seen at the angle (2θ) 23.35 and its crystallinity index was 3.22%. The crystalline region of insulin loaded Mh2A hydrogel was seen at the angle (2θ) 22.89, and its crystallinity index was 3.32%. The crystalline region of insulin

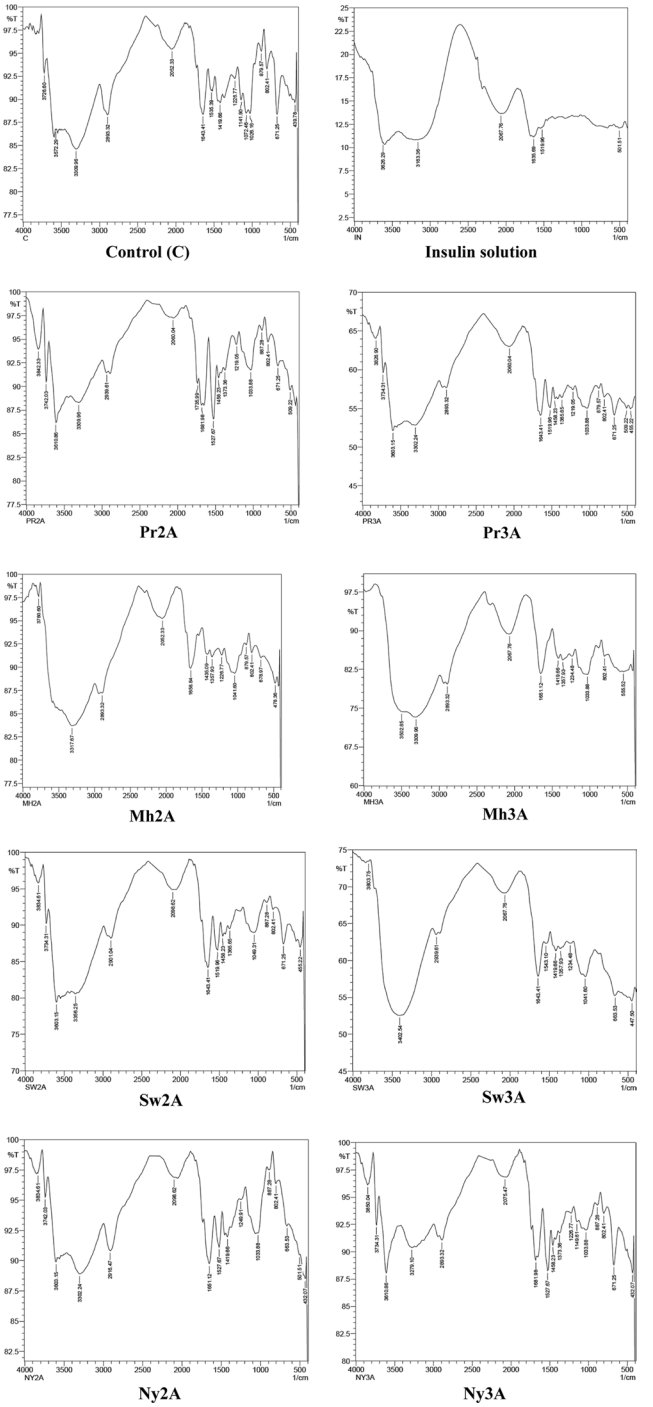

Fig. 6 FTIR spectra of insulin solution and drug (Insulin) loaded hydrogels prepared from polysaccharide isolated from different *Cyamopsis tetragonoloba* L. varieties

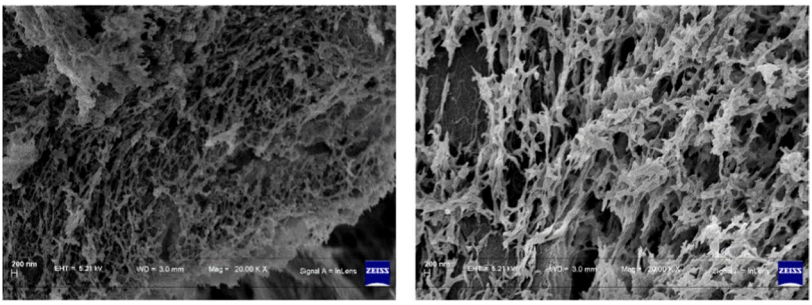

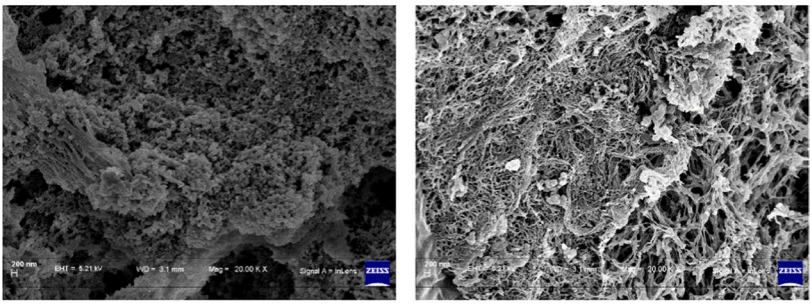

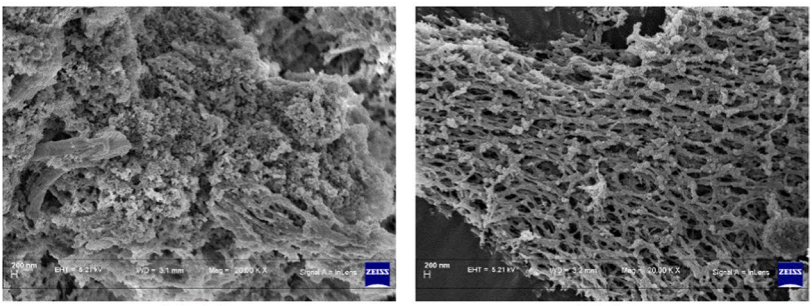

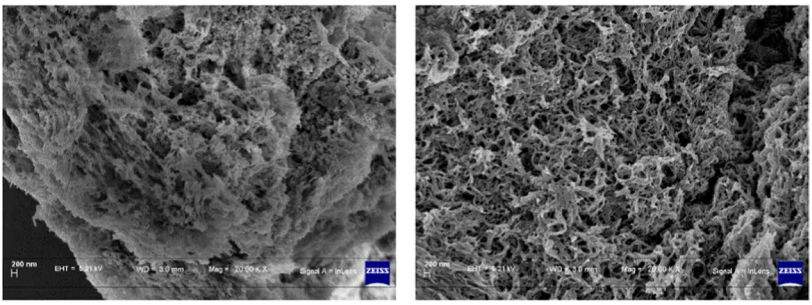

Fig. 7 FESEM of drug (Insulin) loaded hydrogels prepared from polysaccharide isolated from different *Cyamopsis tetragonoloba* L. varieties

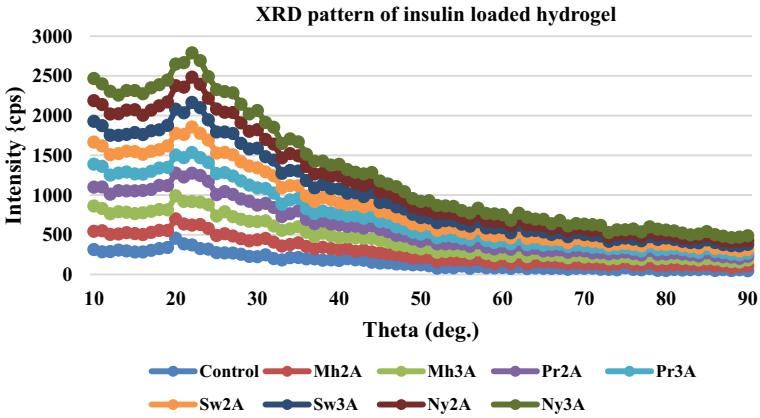

Fig. 8 XRD pattern of the drug (Insulin) loaded hydrogels prepared from polysaccharides isolated from different *Cyamopsis tetragonoloba* L. varieties

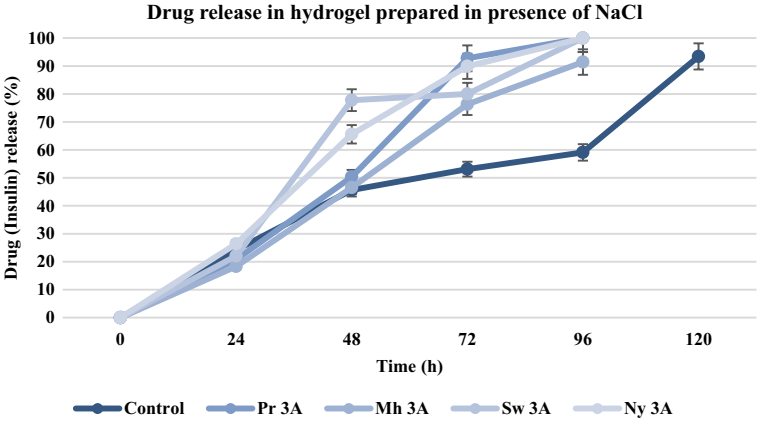

Fig. 9 Drug release in hydrogel prepared in presence of NaCl

loaded Mh3A hydrogel was seen at the angle (2θ) 22.66, and its crystallinity index was 3.02%. The crystalline region of insulin loaded Sw2A hydrogel was seen at the angle (2θ) 22.89, and its crystallinity index was 3.65%. The crystalline region of insulin loaded Sw3A hydrogel was seen at the angle (2θ) 22.55, and its crystallinity index was 3.89%. The crystalline region of insulin loaded Ny2A hydrogel was seen at the angle (2θ) 22.21, and its crystallinity index was 3.67%. The crystalline region of insulin loaded Ny3A hydrogel was seen at the angle (2θ) 22.32, and its crystallinity index was 3.31%. The diffraction pattern of all the drug-loaded hydrogels was similar to each other with no difference in the intensities of insulin or galactomannan peaks (Fig. 8). This suggests that the insulin is stable and underwent amorphous dispersion within the galactomannan hydrogel.

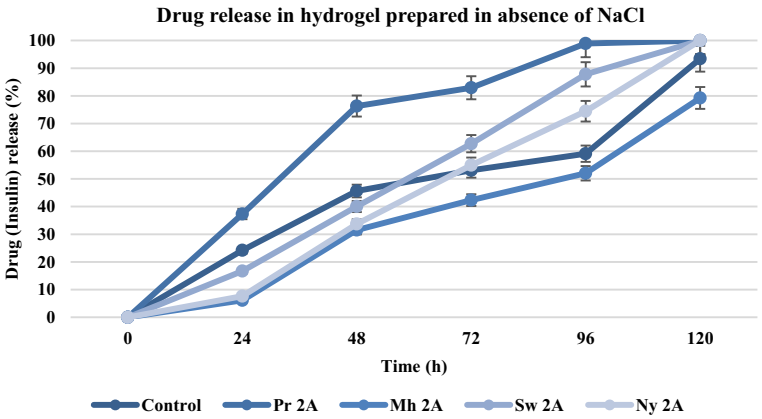

Fig. 10 Drug release in hydrogel prepared in absence of NaCl

In vitro drug release and assessment of drug release kinetics

From the in vitro drug release studies, it was observed that the controlled drug release was observed in hydrogels prepared in absence of NaCl as compared to hydrogels prepared in presence of NaCl (Figs. 9 and 10). For evaluation of drug release kinetics, the various kinetic models (Zero order, First order, Higuchi, Hixson-Crowell, and Korsmeyer-Peppas were used using DD solver software. From the different kinetic modeling analyses, it was observed that there was a significant controlled release of drug observed in hydrogels prepared from galactomannan of Parasiya 954 (Pr 2A), Maharani 92 (Mh 2A), Swati (Sw 2A) and Nylon 55 (Ny 2A) varieties in absence of NaCl with correlation coefficient 0.9449 to 0.9998. However, no significant controlled release of drug was observed in hydrogels prepared from galactomannan of Parasiya 954 (Pr 3A), Swati (Sw 3A) and Nylon 55 (Ny 3A) varieties in presence of NaCl with a correlation coefficient of 0.006 to − 0.08. Remarkably significant controlled release of insulin was observed in hydrogel prepared from galactomannan of Maharani 92 (Mh 3A) variety in presence of NaCl with a correlation coefficient of 0.99 (Tables 5 and 6 Supplementary data).

From the release rate analysis of all the formulations through different kinetics models, it was observed that the values of n for formulations (Control, Pr 2A, Mh 2A, Sw 2A, Ny 2A, and Mh 3A) are in the range between 0.5 and 1.33 which indicated non-Fickian diffusion. However, the values of n for formulations Pr 3A, Sw 3A, Ny 3A is less than 0.1 which indicated Ficklan diffusion of drug [56, 57]. The significant controlled drug release was observed in hydrogels prepared in absence of NaCl due to ionization of hydroxyl groups of boric acid. In the hydrogels, ionization of hydroxyl group increases swelling property and hydration which in turn enhances drug release. However, an increase in the cross-linking agent (NaCl) decreases the porosity, swelling, and hydration of gel which inhibits the interaction of drug molecules with the physiological medium and decreases the drug release [20].

Statistical analysis of data

Multivariate cluster analysis was used to detect the similarity in the characteristics of all the twelve hydrogels prepared from different varieties of *Cyamopsis tetragonoloba* L. in the presence or absence of NaCl. The Cluster analysis grouped the twelve hydrogels prepared either in the presence or absence of NaCl into major two groups on the basis of their qualitative and quantitative characteristics (Yield of hydrogel, water-holding capacity, swelling property, sol–gel fraction, porosity, and drug loading capacity). Group A included hydrogels (D2A, D3A, Nm2A, Nm3A) prepared from *Desi* and *Neelam 51* variety that correspond to the particulate matter, no water-holding capacity, no intactness or stickyness, no swelling property and no drug loading capacity. Group B included hydrogels (Mh2A, Mh3A, Pr2A, Pr3A, Sw2A, Sw3A, Ny2A, Ny3A) prepared from and Maharani 92, Parasiya 954, Swati and Nylon 55 varieties that correspond to the formation of intact hydrogel, have water-holding capacity, have swelling property, and have drug loading capacity. Among them, the hydrogels Mh3A, Pr3A, Pr2A, Sw2A, and Ny2A were similar to each other with moderate water-holding capacity, intact and sticky gel, high swelling property, high gel fraction, high porosity, and high drug loading capacity. The hydrogels Sw3A and Ny3A were similar to each other with high water-holding capacity, intact and sticky gel, high swelling property, high gel fraction, low

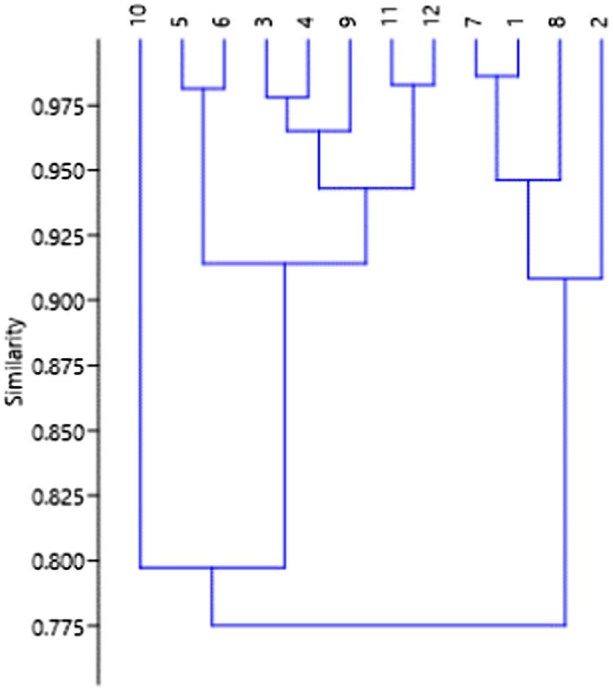

Fig. 11 Dendrogram based on the Paired group (UPGMA) algorithm using similarity index Bray–Curtis for clustering of twelve hydrogels [1) D3A 2) Nm3A 3) Pr3A 4) Mh3A 5) Sw3A 6) Ny3A 7) D2A 8) Nm2A 9) Pr2A 10) Mh2A 11) Sw2A 12) Ny2A] on the basis of quantitative and qualitative parameters

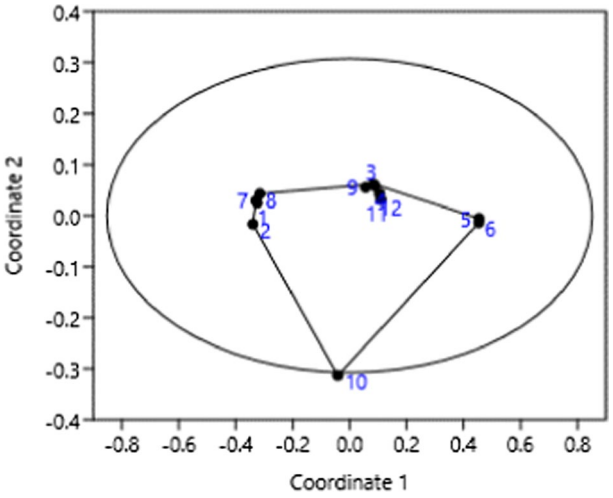

Fig. 12 The non-metric multidimensional scaling of twelve hydrogels [1) D3A 2) Nm3A 3) Pr3A 4) Mh3A 5) Sw3A 6) Ny3A 7) D2A 8) Nm2A 9) Pr2A 10) Mh2A 11) Sw2A 12) Ny2A] for clustering on the basis of quantitative and qualitative parameters

porosity, and high drug loading capacity. The hydrogel Mh2A was different from all the hydrogels with high water-holding capacity, watery intact gel, high swelling property, high gel fraction, high porosity, and high drug loading capacity. Similar clusters were also formed by non-metric multidimensional scaling (MDS) (Figs. 11 and 12) which supports the results of multivariate Cluster analysis.

Conclusions

From the present studies, it was concluded that characteristics of isolated galactomannan and physiological properties of prepared hydrogels from Desi and Neelam 51 variety, Parasiya 954 and Maharani 92 variety, and Swati and Nylon 55 were similar to each other, respectively. The hydrogel formation was not observed in Desi and Neelam variety but it formed particulate matter. The hydrogel formed from Parasiya 954 and Maharani 92 variety was sticky watery gel whereas hydrogel formed from Swati and Nylon 55 variety was intact and sticky gel. The physiological properties (very watery gel, thick watery gel, thick intact gel) of hydrogels can be varied by changing the pH of the formulations prepared in absence of NaCl which cannot be altered in formulations prepared in presence of NaCl. The steady shear flow curve of intact hydrogels (Pr2A, Mh2A, Sw2A, Ny2A) suggested that they had shear-thinning behavior. The viscosity of all hydrogels suggested that they had Newtonian behavior which indicates the weak and flexible structure of hydrogels. From the amplitude sweep studies, it was observed that all the hydrogels (C, Pr2A, Mh2A, Sw2A, & Ny2A) behaved as dilatant shear thickening fluid. From the frequency sweep studies, it was observed that the strength of Ny2A and Sw2A hydrogels is high as compared to C, Pr2A, and Mh2A. The FTIR and FESEM analysis

of drug-loaded hydrogels confirmed the formation of polymerization in intact and sticky hydrogels, porous morphology, and entrapment of insulin in hydrogels. The FTIR and XRD analysis of drug-loaded hydrogels revealed that the stable structure of insulin was retained and its amorphous dispersion in hydrogels, respectively. The controlled drug (insulin) release was observed in formulations C, Pr 2A, Mh 2A, Sw 2A, Ny 2A, and Mh 3A with non-Fickian diffusion of the drug. However, controlled release was not observed in formulations Pr 3A, Sw 3A, Ny 3A with Ficklan diffusion of drug.

Supplementary Information The online version contains supplementary material available at https://doi.org/10.1007/s00289-022-04483-w.

Acknowledgments The authors wholeheartedly thank and appreciate the support given by the Department of Biosciences, Department of Chemistry SAIF facility, National Facility for Drug Discovery, Center of excellence, Saurashtra University, and CSIR-CSMCRI, Bhavnagar to carry out the present research work.

Author contributions SA performed experiments for this research work as a part of her Ph.D thesis. JGT contributed to experiment design, standardization of experiments, data analysis, interpretation of results, and manuscript preparation.

Funding Authors are wholeheartedly thankful to State Government of Gujarat, India for Shodha Fellowship given to Ph.D student to carry out the present research work.

Data availability Data are included in the form of tables and figures.

Declarations

Conflict of interest Authors declare that there is no conflict of interest regarding publication of this research article in journal.

Consent for publication Authors give consent for publication of this research work in your esteemed journal.

Ethical approval No ethical approval is required for this present research work.

Consent to participate Authors declare to participate for the publication of this research work in your esteemed journal

References

1. Liyanage S, Abidi N, Auld D et al (2015) Chemical and physical characterization of galactomannan extracted from guar cultivars (*Cyamopsis tetragonolobus* L.). Ind Crops Prod 74:388–396
2. Srivastava M, Kapoor VP (2005) Seed galactomannans: an overview. Chem Biodivers 2(3):295–317
3. Prajapati VD, Jani GK, Moradiya NG et al (2013) Galactomannan: a versatile biodegradable seed polysaccharide. Int J Biol Macromol 60:83–92
4. Thakura S, Sharma B, Verma A et al (2018) Recent approaches in guar gum hydrogel synthesis for water purification. Int J Polym Anal Charact 23(7):621–632
5. Rithe SS, Kadam PG, Mhaske ST (2014) Preparation and analysis of novel hydrogels prepared from the blend of guar gum and chitosan: cross-linked with glutaraldehyde. Adv Mater Sci Eng 2:1–15
6. Elsaeed SM, Zaki EG, Omar WA et al (2021) Guar gum-based hydrogels as potent green polymers for enhanced oil recovery in high-salinity reservoirs. ACS Omega 6(36):23421–23431

7. Chen X, Martin BD, Neubauer TK et al (1995) Enzymatic and chemoenzymatic approaches to synthesis of sugar based polymer and hydrogels. Carbohydr Polym 28:15–21
8. Kashyap N, Kumar N, Kumar M (2005) Hydrogels for pharmaceutical and biomedical applications. Crit Rev Ther Drug Carr Syst 22:107–149
9. Hamidi M, Azadi A, Rafiei P (2008) Hydrogel nanoparticles in drug delivery. Adv Drug Deliv Rev 60(15):1638–1649
10. Singh A, Sharma PK, Garg VK et al (2010) Hydrogels: a review. Int J Pharm Sci Rev Res 4(2):97–105
11. Zhang L, Li K, Xiao W et al (2011) Preparation of collagen–chondroitin sulfate–hyaluronic acid hybrid hydrogel scaffolds and cell compatibility in vitro. Carbohydr Polym 84(1):118–125
12. Saul JM, Williams DF (2011) Hydrogels in regenerative medicine. Handbook of polymer applications in medicine and medical devices. William Andrew Publishing, pp 279–302
13. Hiremath JN, Vishalakshi B (2012) Effect of crosslinking on swelling behaviour of IPN hydrogels of guar gum & polyacrylamide. Der Pharma Chemica 4(3):946–955
14. Verma D, Sharma SK (2021) Recent advances in guar gum based drug delivery systems and their administrative routes. Int J Biol Macromol 181:653–671
15. Sullad AG, Manjeshwar LS, Aminabhavi TM (2010) Novel pH-sensitive hydrogels prepared from the blends of poly(vinyl alcohol) with acrylic acid-graft-guar gum matrixes for isoniazid delivery. Ind Eng Chem Res 49:7323–7329
16. Soppimath KS, Kulkarni AR, Aminabhavi TM (2000) Controlled release of antihypertensive drug from the interpenetrating network poly (vinyl alcohol)–guar gum hydrogel microspheres. J Biomater Sci Polym Ed 11(1):27–43
17. Palem RR, Shimoga G, Rao KSV et al (2020) Guar gum graft polymer-based silver nanocomposite hydrogels: synthesis, characterization and its biomedical applications. J Polym Res 27(3):1–20
18. Kumar B, Murali A, Bharath AB et al (2019) Guar gum modified upconversion nanocomposites for colorectal cancer treatment through enzyme-responsive drug release and NIR-triggered photodynamic therapy. Nanotechnology 30(31):315102
19. Chen LG, Liu ZL, Zhuo RX (2005) Synthesis and properties of degradable hydrogels of konjac glucomannan grafted acrylic acid for colon-specific drug delivery. Polymer 46(16):6274–6281
20. Bashir S, Teo YY, Ramesh S et al (2016) Synthesis, characterization, properties of N-succinyl chitosan-g-poly (methacrylic acid) hydrogels and in vitro release of theophylline. Polymer 92:36–49
21. Takehara H, Hadano Y, Kanda Y, Ichiki T (2020) Effect of the thermal history on the crystallinity of poly (L-lactic Acid) during the micromolding process. Micromachines 11(5):452
22. Paixão MVG, de Carvalho BR (2018) Application of guar gum in brine clarification and oily water treatment. Int J Biol Macromol 108:119–126
23. Shabir F, Erum A, Tulain UR et al (2017) Preparation and characterization of pH sensitive crosslinked Linseed polysaccharides-co-acrylic acid/methacrylic acid hydrogels for controlled delivery of ketoprofen. Des Monomers Polym 20(1):485–495
24. Gulrez SK, Al-Assaf S, Phillips GO (2011) Hydrogels: methods of preparation, characterisation and applications. In: Progress in molecular and environmental bioengineering-from analysis and modeling to technology applications, pp 117–150
25. Nagasawa N, Yagi T, Kume T et al (2004) Radiation crosslinking of carboxymethyl starch. Carbohydr Polym 58(2):109–113
26. Lin WJ, Lu CH (2002) Characterization and permeation of microporous poly (ε-caprolactone) films. J Membr Sci 198(1):109–118
27. Ranjha NM, Hanif M, Afzal Z et al (2015) Diffusion coefficient, porosity measurement, dynamic and equilibrium swelling studies of Acrylic acid/Polyvinyl alcohol (AA/PVA) hydrogels. Pak J Pharm Res 1(2):48–57
28. Kokol V, Pottathara YB, Mihelčič M et al (2021) Rheological properties of gelatine hydrogels affected by flow-and horizontally-induced cooling rates during 3D cryo-printing. Colloids Surf A Physicochem Eng Asp 616:126356
29. Abd El-Mohdy HL, Hegazy EA, El-Nesr EM et al (2016) Synthesis, characterization and properties of radiation-induced Starch/(EG-co-MAA) hydrogels. Arab J Chem 9:S1627–S1635
30. Shah N, Patel K (2014) Formulation and development of hydrogel for poly acrylamide-co-acrylic acid. J Pharm Sci Biosci Res Patel 4:114–120

31. Bradford MM (1976) A rapid and sensitive method for the quantitation of microgram quantities of protein utilizing the principle of protein-dye binding. Anal Biochem 72(1–2):248–254
32. Hammer Ø, Harper DA, Ryan PD (2001) PAST: paleontological statistics software package for education and data analysis. Palaeontol Electron 4(1):9
33. Mudgil D, Barak S, Khatkar BS (2012) X-ray diffraction, IR spectroscopy and thermal characterization of partially hydrolyzed guar gum. Int J Biol Macromol 50(4):1035–1039
34. Warrand J, Michaud P, Picton L et al (2005) Structural investigations of the neutral polysaccharide of *Linum usitatissimum* L. seeds mucilage. Int J Biol Macromol 35(3–4):121–125
35. Kačuráková M, Belton PS, Wilson RH et al (1998) Hydration properties of xylan-type structures: an FTIR study of xylooligosaccharides. J Sci Food Agric 77(1):38–44
36. Kačuráková M, Ebringerova A, Hirsch J et al (1994) Infrared study of arabinoxylans. J Sci Food Agric 66(3):423–427
37. Thombare N, Mishra S, Siddiqui MZ et al (2018) Design and development of guar gum based novel, superabsorbent and moisture retaining hydrogels for agricultural applications. Carbohydr Polym 185:169–178
38. Fringant C, Tvaroska I, Mazeau K et al (1995) Hydration of α-maltose and amylose: molecular modelling and thermodynamics study. Carbohydr Res 278(1):27–41
39. Mudgil D, Barak S, Khatkar BS (2012) Effect of enzymatic depolymerization on physicochemical and rheological properties of guar gum. Carbohyd Polym 90(1):224–228
40. Tayal A, Pai VB, Khan SA (1999) Rheology and microstructural changes during enzymatic degradation of a guar−borax hydrogel. Macromolecules 32(17):5567–5574
41. Jafry HR, Pasquali M, Barron AR (2011) Effect of functionalized nanomaterials on the rheology of borate cross-linked guar gum. Ind Eng Chem Res 50(6):3259–3264
42. Bishop M, Shahid N, Yang J et al (2004) Determination of the mode and efficacy of the crosslinking of guar by borate using MAS 11B NMR of borate cross-linked guar in combination with solution 11B NMR of model systems. Dalton Trans 17:2621–2634
43. Mesmer RE, Baes CF, Sweeton FH (1972) Acidity measurements at elevated temperatures: VI. Boric acid equilibriums. Inorg Chem 11:537–543
44. Wang S, Tang H, Guo J et al (2016) Effect of pH on the rheological properties of borate crosslinked hydroxypropyl guar gum hydrogel and hydroxypropyl guar gum. Carbohydr Polym 147:455–463
45. Harris PC (1993) Chemistry and rheology of borate-crosslinked fluids attemperatures to 300 F. J Pet Technol 45:264–269
46. Sharma K, Kumar V, Chaudhary B et al (2016) Application of biodegradable superabsorbent hydrogel composite based on Gum ghatti-co-poly (acrylic acid-aniline) for controlled drug delivery. Polym Degrad Stab 124:101–111
47. Amin MCIM, Ahmad N, Halib N et al (2012) Synthesis and characterization of thermo-and pH-responsive bacterial cellulose/acrylic acid hydrogels for drug delivery. Carbohydr Polym 88(2):465–473
48. Zhang J, Chu LY, Cheng CJ et al (2008) Graft-type poly (N-isopropylacrylamide-co-acrylic acid) microgels exhibiting rapid thermo-and pH-responsive properties. Polymer 49(10):2595–2603
49. Mahdavinia GR, Pourjavadi A, Hosseinzadeh H et al (2004) Modified chitosan 4. Superabsorbent hydrogels from poly (acrylic acid-co-acrylamide) grafted chitosan with salt-and pH-responsiveness properties. Eur Polym J 40(7):1399–1407
50. Ranjha NM, Qureshi UF (2014) Preparation and characterization of crosslinked acrylic acid/hydroxypropyl methyl cellulose hydrogels for drug delivery. Int J Pharm Pharm Sci 6(4):400–410
51. Pourjavadi A, Barzegar S, Mahdavinia GR (2006) MBA-crosslinked Na-Alg/CMC as a smart full-polysaccharide superabsorbent hydrogels. Carbohydr Polym 66(3):386–395
52. Ranjha NM, Ayub G, Naseem S et al (2010) Preparation and characterization of hybrid pH-sensitive hydrogels of chitosan-co-acrylic acid for controlled release of verapamil. J Mater Sci Mater Med 21(10):2805–2816
53. Soleimani F, Sadeghi M (2012) Synthesis of pH-sensitive hydrogel based on starch-polyacrylate superabsorbent. J Biomater Nanobiotechnol 3(2A):310–314
54. Highley CB, Rodell CB, Burdick JA (2015) Direct 3D printing of shear-thinning hydrogels into self-healing hydrogels. Adv Mater 27(34):5075–5079
55. Sittikijyothin W, Sampaio P, Goncalves MP (2007) Heat-induced gelation of-lactoglobulin at varying pH: effect of tara gum on the rheological andstructural properties of the gels. Food Hydrocoll 21:1046–1055

56. Ritger PL, Peppas NA (1987) A simple equation for description of solute release I. Fickian and non-fickian release from non-swellable devices in the form of slabs, spheres, cylinders or discs. JCR 5(1):23–36
57. Ritger PL, Peppas NA (1987) A simple equation for description of solute release II. Fickian and anomalous release from swellable devices. JCR 5(1):37–42